University of Hamburg • Institute of Oceanography • Remote Sensing

SOPRAN 4.4

Global CO_2 Fluxes Derived From Satellite Data

Iris Hinrichs, Martin Gade, and Detlef Stammer

Abstract

Time series of gas transfer velocities, k, derived from scatterometer wind speeds, u_{10}, are presented. The adaption of the k - u_{10} parameterization to the wind products according to Naegler (2009) avoids discontinuities in the time series due to differences between the scatterometer wind products. Estimation of global ocean-atmosphere carbon fluxes was extended by implementing ΔpCO2 maps published by Takahashi et al. (2009). Although consistent on a global scale, the estimated net fluxes show differences on regional scales due to wind speed product differences and different temporal resolutions.

Multi³Scat measurements on FINO 2 have been performed since August 2008, intermitted by system maintenance and technical improvements in Hamburg from May thru November 2009. Our backscatter time series clearly show a modulation by long swell, and strong bursts and a broadened Doppler signal due to wave breaking. In order to interpret and analyze the data obtained statistically , a metadata base has been set up including concurrent meteorological and hydrological data.

CO_2 Flux Reference Data Set

A reference data set of global CO_2 fluxes has been created using scatterometer wind speed data (ERS-1, ERS-2 and QuikSCAT) and ΔpCO_2 maps for 1995 (Takahashi et al, 2002) and for 2000 (Takahashi et al., 2009). This reference data set will be the basis for analyses of global CO_2 fluxes estimated with an improved parameterization of the gas transfer velocity k: with the help of concurrent measurements of k and radar backscatter (σ^0) from the research platform FINO 2 (see below) a relationship of k and σ^0 shall be found. Since measurements on FINO2 are delayed, the reference data set has been analyzed.
The wind speed products used show spatial differences on regional scales.
The gas transfer velocity can be expressed as a function of wind speed in 10 m height according to

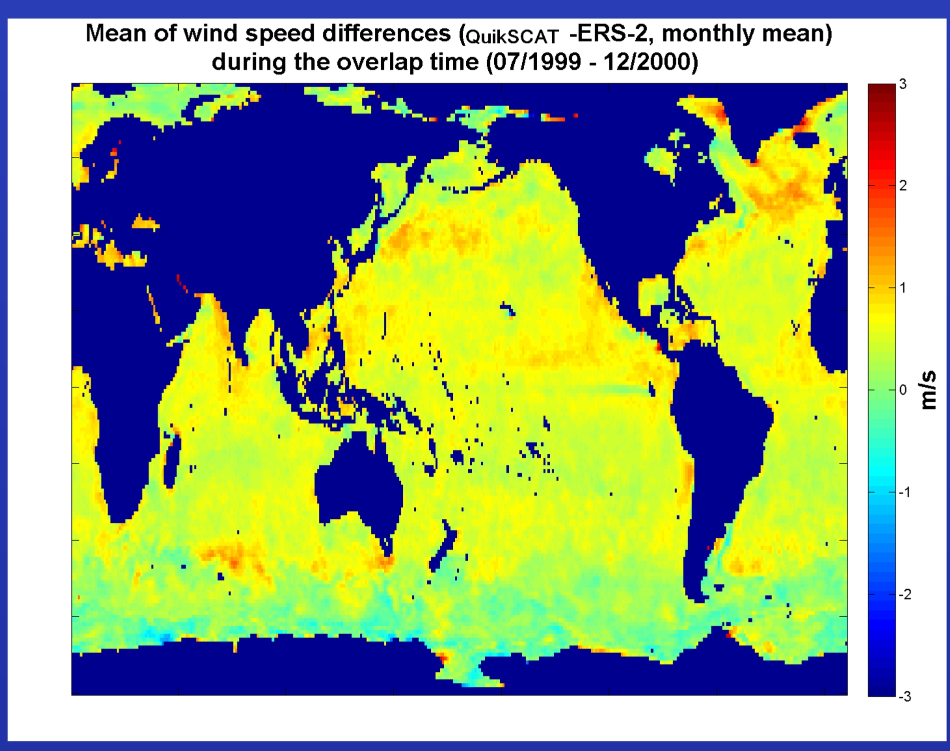

$k = b\,(u_{10})^n\,(Sc/660)^{-0.5}$, n = 1, 2, 3

A linear, quadratic, and cubic parameterization was applied. The figure below shows Hovmöller diagrams of the gas transfer velocity derived from ERS-2 monthly wind speed with the three different parameterizations. It can clearly be seen that a different contrast between areas of high and low wind speeds occurs by applying the parameterizations.

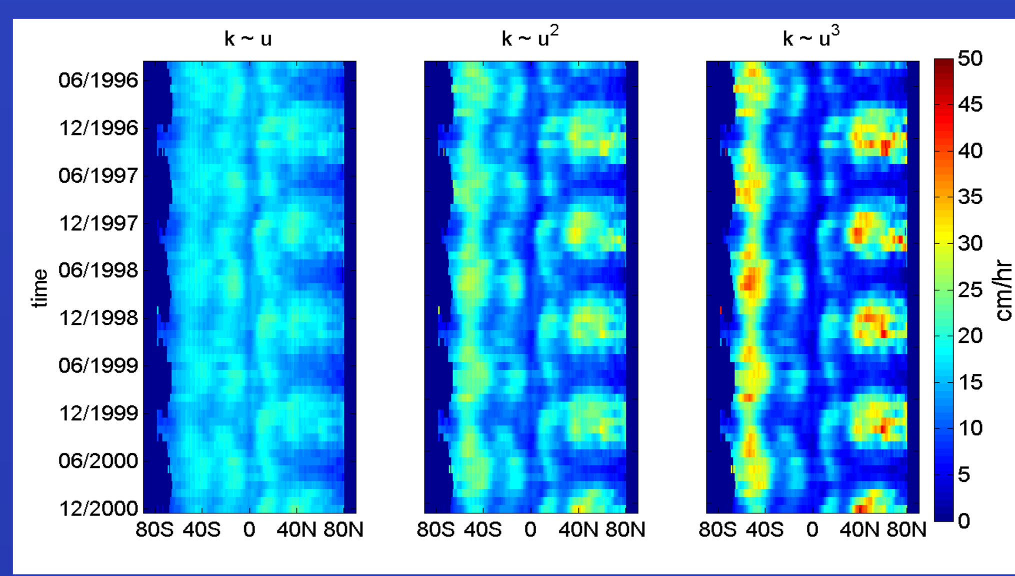

In order to meet the constraint of the global gas transfer velocity derived from the global ^{14}C inventory (k_{glob} = 16.5 cm/h, Nägler 2009), the applied parameterizations are tuned to the respective wind speed product.
Concerning the global CO_2 fluxes (see upper right panel) the tuning to the global mean gas transfer velocity could compensate for the differences in the wind speed product. Here, neither the temporal resolution nor the choice of the wind speed product, nor the applied ΔpCO_2 data set cause significant differences in the flux.

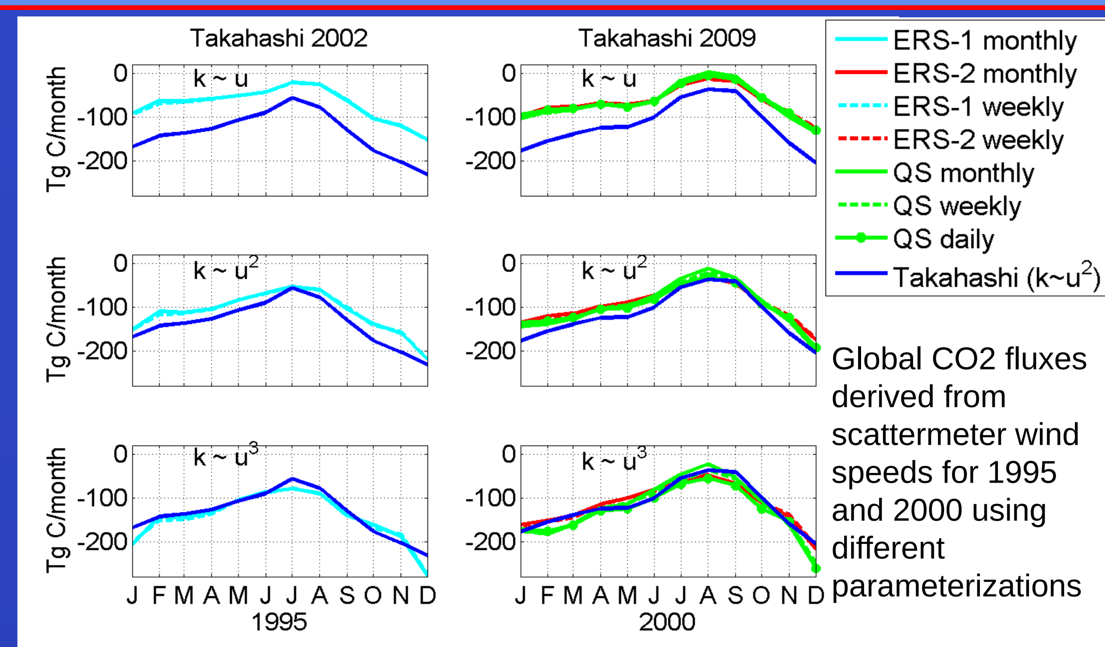

Global CO2 fluxes derived from scatterometer wind speeds for 1995 and 2000 using different parameterizations

However, the choice of parameterization determines the rate of the global flux.
On a regional scale (see lower right panel), however, the choice of wind speed product, ΔpCO_2 data set and temporal resolution do matter.
All these considerations have to be taken into account, when finally applying the k- σ^0 to spaceborne scatterometer data.

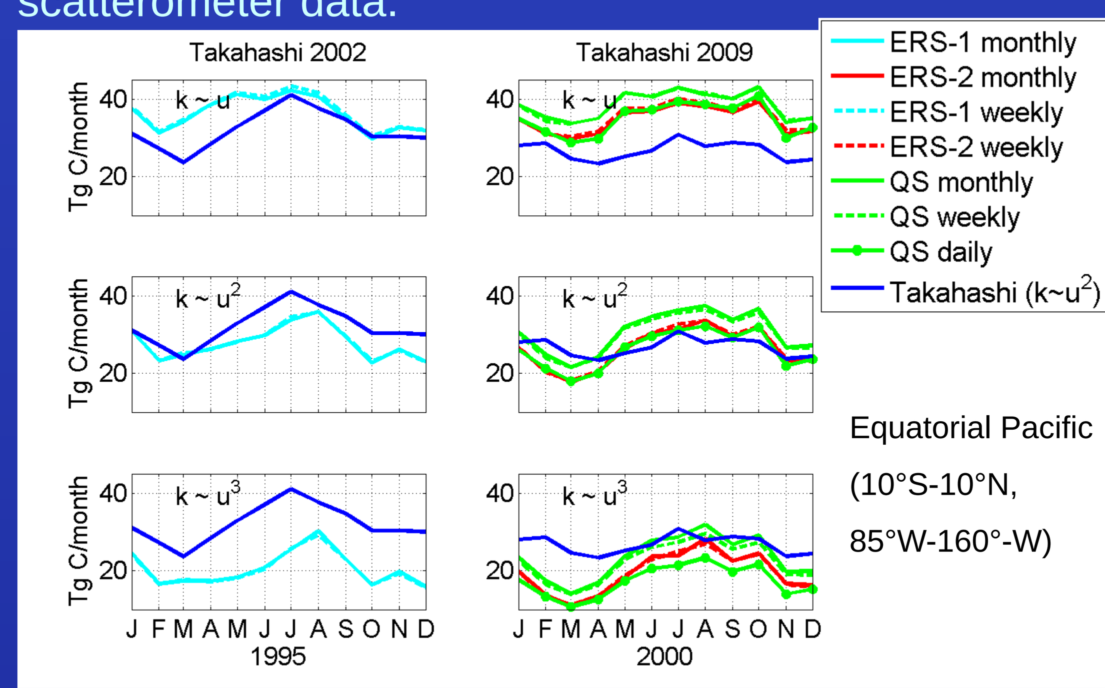

Equatorial Pacific

(10°S-10°N,

85°W-160°-W)

Multi³Scat on FINO-2

Wave breaking enhances the turbulence in the upper water layer, produces air bubbles, and therefore increases the gas transfer velocity significantly. Our goal is to identify, and to quantify, breaking wave events through a thorough analysis of the Multi³Scat data from FINO-2. Two spectrograms are shown to demonstrate the effect of wave breaking on the backscattered radar signal. The data were acquired by Multi³Scat at C band, HH polarization, at different wind and wave conditions: From August 12 to 14, the wind speed increased from 7 m/s to 13 m/s (the wind direction was changing only slightly). Along with the increase in wind speed the frequency of wave breaking events increased, thus leading to an increased radar backscatter and Doppler shift.

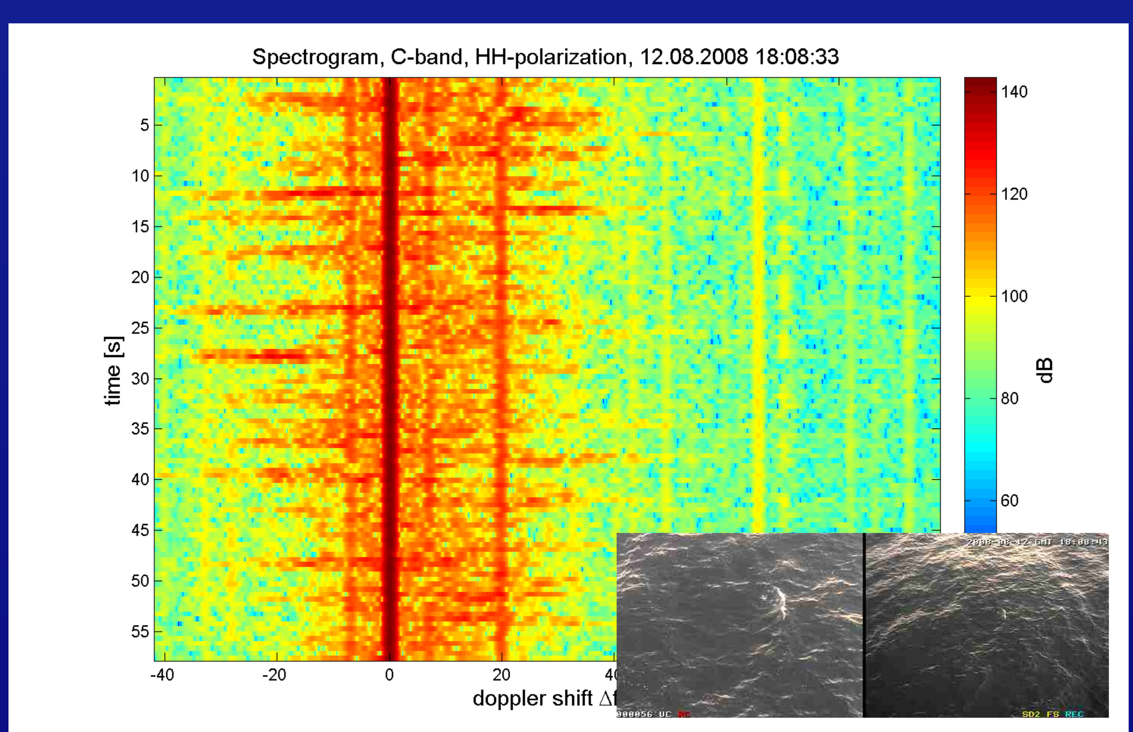

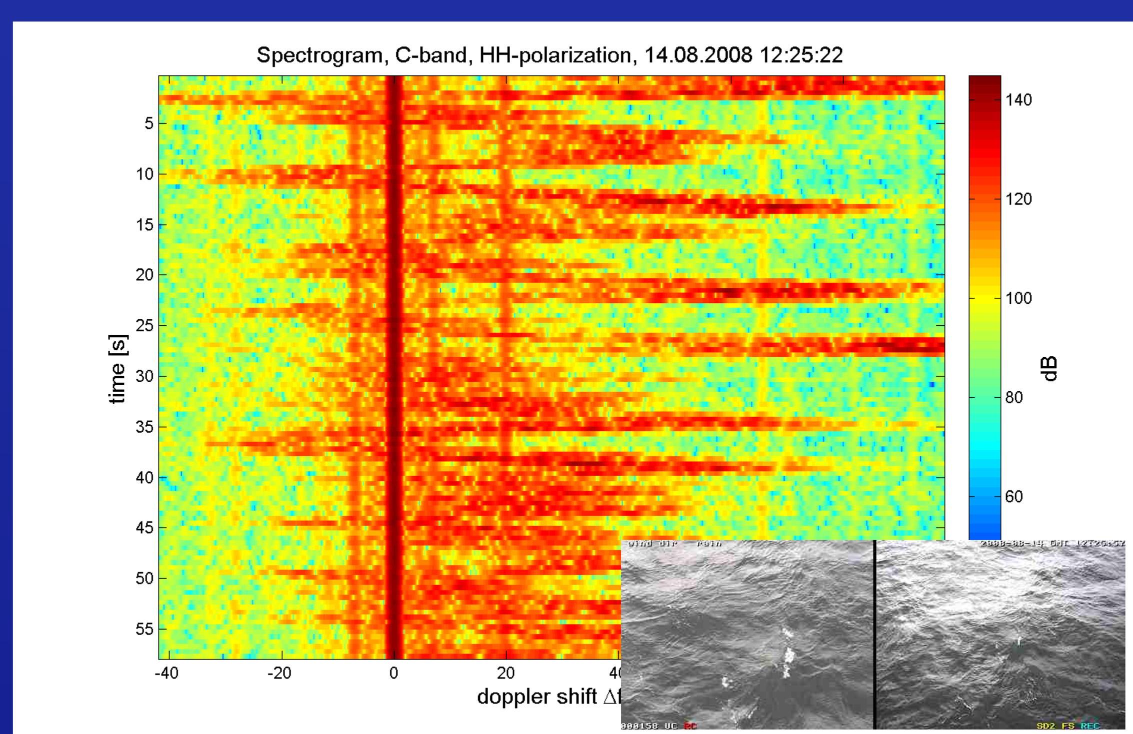

Both wind speed and sea state were moderate on August 12 (lower left panel), resulting in a moderate overall radar backscattering and low Doppler shifts.

On August 14 (upper middle panel), the wind speed was high (13 m/s), but the sea state had grown significantly. As a result, the radar backscattering is strong and a wave-induced undulation can be detected.

Meta data base

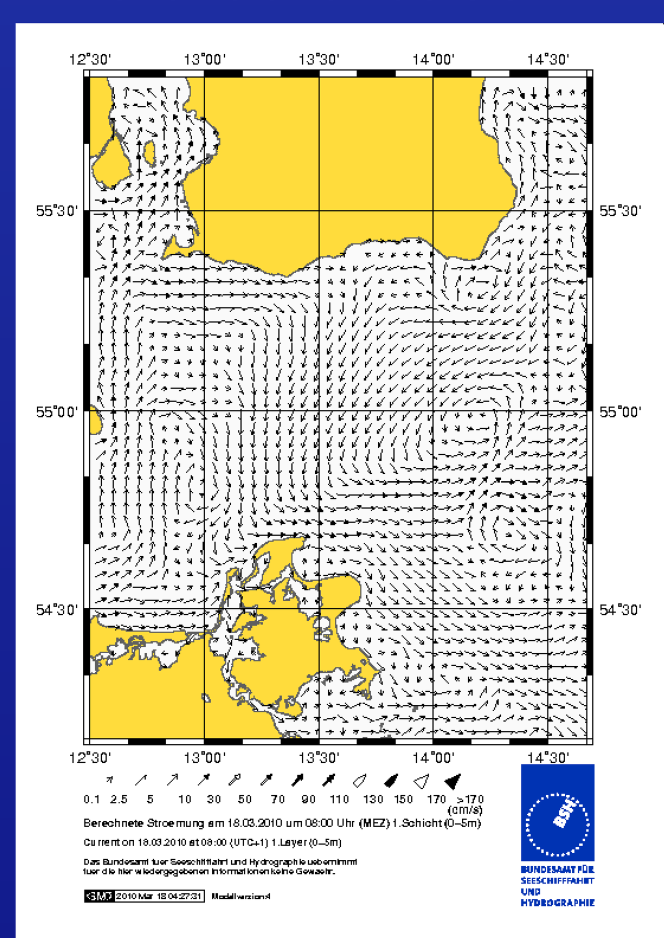

References:

Naegler, T., Reconciliation of excess 14C-constrained global CO2 piston velocity estimates, Tellus B, 2009, pp. 372--384

Takahashi, T., Sutherland, S. C., Sweeney, C., Poisson, A., Metzl, N., Tilbrook, B., Bates, N., Wanninkhof, R., Feely, R. A., Sabine, C., Olafsson, J. and Nojiri, Y. "Global sea-air CO2 flux based on climatological surface ocean pCO2, and seasonal biological and temperature effects," *Deep-Sea Res* (49), 2002, pp. 1601--1622.

Takahashi, Taro and Stewart C. Sutherland and Rik Wanninkhof and Colm Sweeney and Richard A. Feely and David W. Chipman and Burke Hales and Gernot Friederich and Francisco Chavez and Christopher Sabine and Andrew Watson and Dorothee C.E. Bakker and Ute Schuster and Nicolas Metzl and Hisayuki Yoshikawa-Inoue and Masao Ishii and Takashi Midorikawa and Yukihiro Nojiri and Arne Körtzinger and Tobias Steinhoff and Mario Hoppema and Jon Olafsson and Thorarinn S. Arnarson and Bronte Tilbrook and Truls Johannessen and Are Olsen and Richard Bellerby and C.S. Wong and Bruno Delille and N.R. Bates and Hein J.W. de Baar, Climatological mean and decadal change in surface ocean pCO2, and net sea-air CO2 flux over the global oceans, Deep Sea Research Part II: Topical Studies in Oceanography, 2009, pp. 554 - 577